Microelectronic Engineering 115 (2014) 55–60

Contents lists available at ScienceDirect

Microelectronic Engineering

journal homepage: www.elsevier.com/locate/mee

1-D polymeric photonic crystals as spectroscopic zero-power humidity sensors

M.-I. Georgaki [a,b], A. Botsialas [a], P. Argitis [a], N. Papanikolaou [a], P. Oikonomou [a], I. Raptis [a,c], J. Rysz [d], A. Budkowski [d], M. Chatzichristidi [a,b,*]

[a] Department of Microelectronics, Institute of Advanced Materials Physicochemical Processes Nanotechnology and Microsystems, NCSR 'Demokritos', Athens, Greece
[b] Department of Chemistry, University of Athens, Athens, Greece
[c] ThetaMetrisis S.A., Polydefkous 14, 12243 Athens, Greece
[d] M. Smoluchowski Institute of Physics, Jagiellonian University, Reymonta 4, Kraków, Poland

ARTICLE INFO

Article history:
Received 22 July 2013
Received in revised form 1 November 2013
Accepted 6 November 2013
Available online 16 November 2013

Keywords:
Polymer photonic crystal
Color humidity Sensor
Photolithography

ABSTRACT

In the present study, a one dimensional polymeric photonic crystal is designed, fabricated and evaluated as a humidity sensor. The polymeric photonic crystal is consisted of a multilayer stack of sequential hydrophobic and hydrophilic layers applied using conventional photolithographic steps: spin-coating and DUV exposure. During exposure in a humidity environment, the hydrophilic layers of the sensor swell, hence growing its optical path and giving a red-shift of the reflectance peak and consequently a different color of the device. The spectroscopic humidity sensor does not require external power since its sensing ability is based on the reflectance peak shift of the photonic crystal in the visible spectrum (color change of the sensor). The design, fabrication, evaluation and characterization of the device and its evaluation as humidity sensor is presented.

1. Introduction

Photonic crystals (PC) are periodic dielectric or metal-dielectric nanostructures that affect the propagation of the light depending on its wavelength [1,2]. These periodic structures of high and low refractive index regions have already shown numerous interesting optical properties and their application has been suggested for a wide range of diverse applications such as low and high reflection coatings on lenses and mirrors, color changing paints, and photonic crystal fibers [3–9]. Photonic crystals are either 1-D, 2-D or 3-D with the 1-dimensional (1-D) configuration be the simplest one. The 1-D PC is a multilayer stack of two alternating transparent materials with different refractive indices (low refractive index, marked as material-A and high refractive index marked as material-B throughout the manuscript). Such 1-D PC acts as Bragg mirror, Fig. 1, and upon illumination with broad-band light a particular reflectance spectrum with narrow-band and high reflectance spectral region is observed whereas all other wavelengths are highly transmitted through the multilayer stack. The optical properties of the 1-D PC depend on film thicknesses, refractive indices of materials A and B, number of alternating bilayers, layer thickness uniformity, interfaces quality etc. [2].

When assuming the ideal configuration of perfect thickness uniformity in all A-layers and B-layers, the central wavelength (λ_0) of the high reflectance band is calculated from the Bragg-reflection equation:

$$\lambda_0 = 2(n_A d_A + n_B d_B)/M \quad (1)$$

where M is the order ($M = 1$ for the first order), n_A and n_B are the real parts of the refractive indices and d_A, d_B the thicknesses of the two repeating layers from materials A and B respectively. The refractive index contrast ($n_B - n_A$) defines the width of the reflectance spectral region and the reflectance intensity through the following equation:

$$\Delta\lambda_0 = 4\lambda_0/\pi * \arcsin[(n_B - n_A)/(n_B + n_A)] \quad (2)$$

where $\Delta\lambda_0$ is the bandwidth of the photonic stopband and for infinite number of bilayers.

The increase of the number of bilayers in a photonic crystal increases its reflectivity and increasing the refractive index contrast between the materials increases both the reflectivity and the bandwidth. In general, high refractive index contrast, ($n_B - n_A$), allows for reflectance peaks of high intensity with a small number of repeating layers and larger width of the high-reflectance spectral region. Furthermore once the technology for the fabrication of 1-D PC is available, more complex structures, such as Fabry–Perot devices, could be realized providing additional functionalities and potential application in other areas.

* Corresponding author at: Department of Chemistry, University of Athens, Athens, Greece. Tel.: +30 2107274335; fax: +30 2107221800.
E-mail address: mchatzi@chem.uoa.gr (M. Chatzichristidi).

0167-9317/$ - see front matter © 2013 Elsevier B.V. All rights reserved.
http://dx.doi.org/10.1016/j.mee.2013.11.003

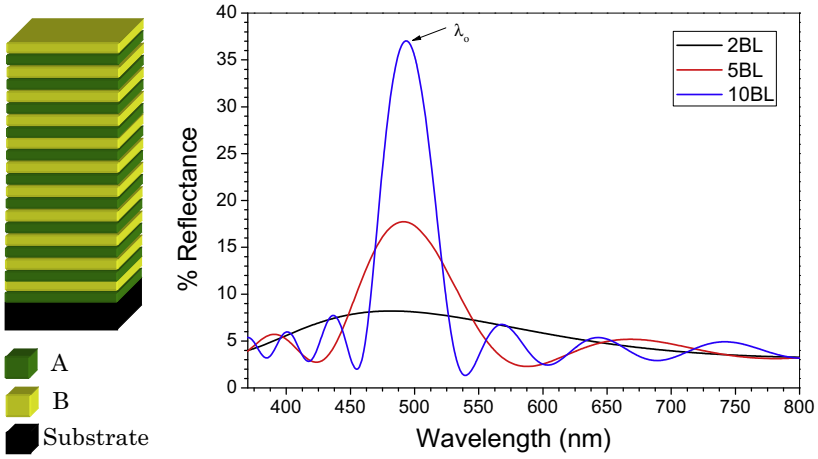

Fig. 1. Theoretical reflectance spectrum from a 2, 5 and 10 bilayer stack of film A with refractive index 1.45 and thickness 90 nm and film B with refractive index 1.65 and thickness 70 nm deposited on glass. On the left side is a schematically representation of a 10 bilayer stack of layers A and B is depicted.

A wide range of 1-D PCs has been fabricated and reported in the literature so far, by employing various transparent materials with research emphasis in materials with high refractive index contrast, $n_B - n_A$, in order to achieve high reflectance value with small number of bilayers. Typical materials in this direction are SiO_2, TiO_2, and polymers that are deposited either via sputtering, sol-gel, spin-coating or co-extrusion. Amongst them, polymers are receiving considerable attention as components in novel 1-D PC because of the tailored functionality, easy deposition, and relatively low cost in most cases of the commercially available ones. The first polymeric 1-D PCs were fabricated by co-extrusion resulting in hundreds to thousands of alternating layers with thickness spanning from the nanoscale to the microscale in a single, one-step roll-to-roll process [10,11]. Recently, several research groups are fabricating 1-D PCs with conventional film deposition techniques (spin-coating [12–14], vapour deposition [15], *etc.*) as well as more sophisticated methods like self-assembled block copolymer [16]. For example, Wang et al. fabricated a photonic paper [17]. They alternately spin coated 26 layers of poly(methyl methacrylate) (PMMA) and poly(N-isopropyl acrylamide-co-glycidyl methacrylate) (PNIPAM-co-PGMA) on a silicon wafer. Then, they exposed the wafer through a patterned mask in order to crosslink the exposed areas of the PNIPAM-co-PGMA films. The fabricated photonic paper showed no color on air due to the low refractive index contrast of the polymers, but when they immersed it in water, the photonic paper gain color from the absorbance of the water molecules from the PNIPSM-co-PGMA films. In addition, the crosslink areas of the PNIPSM-co-PGMA films absorb less water and thus exhibit a different color than the unexposed areas when immersed in water. The photonic paper fabricated can reveal a pre-written pattern (exposed areas) on the wafer by immersion in water.

Another application of 1-D polymeric PC is their use as humidity and volatile organic compounds colorimetric sensors. For example, E. Tian et al. [18] have fabricated a 1-D PC humidity sensor hydrogel by introducing an acrylamide solution into a poly(styrene-methacrylic methacrylate-acrylic acid) PC template and subsequent photo-polymerization. The hydrogel sensor with 20% acrylic acid had a red shift of 100 nm for a humidity change from 20% to 80%.

In the present work a polymeric 1-D PC fabricated by conventional polymeric materials and by employing standard microelectronic processing technologies (spin-coating and lithography), is introduced. In particular, the design, fabrication, characterization and process optimization of 1-D PC is performed along with the evaluation of the device as a spectroscopic zero-power humidity sensor. The finally selected low refractive index material is the hydrophilic poly(2-hydroxyl ethyl methacrylate) (PHEMA) and the high refractive index material is the epoxy based resist EPR ($n_{PHEMA} = 1.51$ and $n_{EPR} = 1.59$ at 632 nm). The fabricated sensor, presents a reflectance peak shift (λ_0) of 62 nm for the transition between 0% and 90% humidity by the application of 10 alternating bilayers. The use of standard polymers and microelectronic processes allow for the fabrication of 1-D PCs on a wide range of substrates such as silicon, glass, flexible substrates. Furthermore the application of the patterning steps allows the definition of 1-D PC areas of any shape with sensing properties or as optical filters.

2. Experimental

Hydrophilic materials absorb water from the environment and swell. Therefore the insertion of a hydrophilic material in a 1-D PC increases the optical path upon humidity due to swelling and results in a red-shift of the reflectance peak, λ_0, according to Eq. (1). Ideally the swelling of the PC would cause spectral shifts in the visible range of the spectra that could be identified by naked eye. The characteristics of colorimetric zero-power humidity sensors based on 1-D PC should be: (a) low cost, (b) easy and repeatable processing, (c) material compatibility (not intermixing between adjacent layers), (d) fast & reversible response and (e) response within the visible spectral range for the whole humidity range. Even though the use of hydrophilic materials for both layers could cause very high swelling upon humidity increase, intermixing might be observed at the interface between adjacent layers that would decrease the sharpness of the refractive index change and therefore affect the reflectance properties of the device. Furthermore the use of two hydrophilic materials could raise processing issues at room conditions since all layers would have been swollen due to the presence of environmental humidity.

In the present study the approach of one hydrophilic and one hydrophobic material was employed since this difference in hydrophobicity facilitate the deposition of subsequent layers with minimal intermixing, if any. Several pairs of hydrophilic/hydrophobic materials were investigated against process compatibility, and swelling due to humidity. The optimum pair in terms of film quality and processing compatibility was found to be poly(2-hydroxy ethyl methacrylate) (PHEMA) [19–21] as hydrophilic material and an Epoxy based resist (EPR) [22,23] as hydrophobic material.

PHEMA is a commercially available hydrophilic methacrylate polymer that produces high quality films via spin-coating [19] and has shown a high humidity sorption either as optical sensor through swelling measurements [24] or chemocapacitive sensor through the change of the dielectric constant [21]. PHEMA is also a lithographic material when exposed at DUV [18]. On the other hand, EPR is a negative tone chemically amplified epoxy based resist that is known to have high hydrophobicity [25] and is easily patterned with standard lithography processing [20,22,26]. Upon exposure and post exposure bake EPR is cross-linked and thus does not dissolve in the PHEMA solvent, turning the two materials orthogonal and suitable for the fabrication of the photonic crystal. The fact that both polymers are patternable could allow for the realization of planar 1-D PC at the desired points and at the shape of interest. The polymer solutions were 3% wt in ethyl lactate for PHEMA and 5% wt in PGMEA for EPR. These concentrations were selected to provide the useful thickness range for each of the films via spin coating. In particular the PHEMA was spin coated at 2000 rpm and post applied baked (PAB) at 110 °C for 5 min on a hotplate while the EPR film was spin coated at 3000 rpm and the same PAB conditions were applied for the fabrication of PHEMA and EPR layers with nominal thickness d_{PHEMA} = 100 nm and d_{EPR} = 70 - nm respectively. The EPR film was then flat exposed at 254 nm with a 500 W Oriel Hg-Xe lamp and post exposure baked (PEB) at 110 °C for 5 min in order to transform the EPR layer to a highly cross-linked film (Cross-EPR). For the formation of the 1-D photonic crystal this bilayer film procedure was repeated several times resulting in a multilayer stack fabrication. The substrates used in the present study were Si wafers, mainly for the characterization of the polymeric films e.g. dissolution, SIMS and quartz wafers for the application of the 1-D PCs.

Dynamic secondary ion mass spectrometry (SIMS) technique was used to investigate multilayer structures. TOF-SIMS 5 (ION-TOF GmbH, Germany) system working in a dual beam mode was used to obtain composition versus depth profiles and 2-dimensional maps of the blend components distribution. Samples were sputtered with C60 ion beam (20 keV, 0.5 nA) rastered over 300 × 300 μm area exposing dipper layers of the film. The structures revealed in the crater centre were analysed with high energy (30 keV) pulsed bismuth beam rastered over 100 × 100 μm. Masses of secondary ions induced by $Bi3^{+}$beam were analyzed in time-of flight mass spectrometer. Intensities of Cl^{-} (m/z = 35), C_2O^{-} (m/z = 40) coming from the polymers, EPR and PHEMA respectively and Si (m/z = 28) from the substrate were normalized by the total ion signal.

3. Results

3.1. Polymer dissolution and interface study

Prior to the fabrication of the 1-D PC, in depth study on the processing effect of each layer to the other (EPR processing on the already deposited PHEMA layer and PHEMA processing on the already deposited Cross-EPR layer) is needed along with characterization of the interface quality in terms of mixing between adjacent layers. The effect of casting solvent of each polymer to the already deposited film of the other polymer is already studied in a previous work of the authors [27] showing that the used combination of polymers is orthogonal.

Another critical characteristic of 1-D PC is the high quality of the interface between the low and high refractive index layers. The minimum intermixing allows for clear transition of the refractive index values and high reflectance values. In the present study, the PHEMA/Cross-EPR and Cross-EPR/PHEMA interfaces quality in terms of intermixing has been investigated by SIMS measurements. In Fig. 2 the SIMS results are presented for a PHEMA/Cross-EPR/PHEMA trilayer.

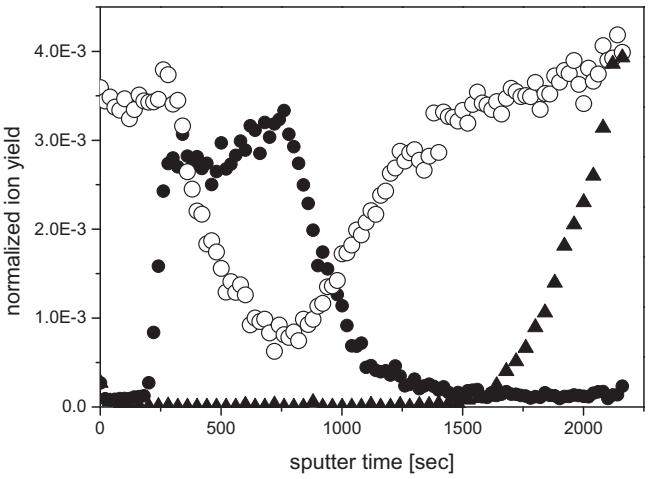

Fig. 2. PHEMA/Cross-EPR/PHEMA trilayer revealed by SIMS depth profiles of: C_2O^{-} (m/z = 40, PHEMA) – open circles, Cl^{-} (m/z = 35, EPR) – solid circles and Si^{-} (m/z = 28, substrate). All signals were normalized by the total ion yield.

3.2. Device fabrication and Film thickness distribution

The results provided so far is a clear prove on the process compatibility and orthogonality of the polymeric films and due to the humidity response performance of PHEMA, the fabrication of a color-based change 1-D photonic crystal can be realizable. The fabrication of the planar device is illustrated in the flow chart of Fig. 3 and constitutes of sequential spin coating and thermal processing steps of PHEMA and EPR films in addition to a UV exposure and thermal processing of the later film in order to crosslinked it, and can be applied on any substrate which in the present study was either Si wafer or microscope glass. Furthermore due to the fact that both PHEMA and EPR act as lithographic materials, it is possible to fabricate a planar 1-D PC of any shape and at the point of interest.

Using the fabrication process illustrated in Fig. 3, multilayer structures can be easily and reproducibly fabricated over large surfaces. Furthermore by tuning the spin coating speed chirped 1-D photonic crystals could be easily fabricated [12]. In Fig. 4 the layer thickness for both polymeric layers for a typical PC consisting of 10 bilayers is illustrated where *X*-axis represents the bilayer number with one being the bilayer adjacent to the substrate and with 10 being the bilayer into contact with the environment. The thickness of each layer is measured with WLRS (FR-Basic VIS by ThetaMetrisis) by considering the film thickness values calculated for the previous layers; i.e. for the calculation of the thickness of the third layer the thickness values for the first layer (PHEMA) and for the second (Cross-EPR) as they were calculated by WLRS just after their deposition and processing are used. The total 1-D PC thickness value is in very good agreement (<2% difference) with the thickness value calculated with stylus profilometry (XP-2 by Ambios). Clearly the thickness for all layers of the same material is not constant and the mean measured thickness was found to be 100 nm ± 5 nm for PHEMA and 70 nm ± 6 nm for Cross-EPR. For comparison in Fig. 5 the experimental (red line) and theoretical (black line) reflectance spectra are illustrated. In the theoretical case, layer thickness was considered equal to the mean value calculated from Fig. 5 results. Furthermore by considering a larger tolerance in film thickness (±15%) of the mean value, the expected reflectance spectrum is illustrated in Fig. 5 (green line). Despite the significant layer thickness variation the reflectance spectrum is in

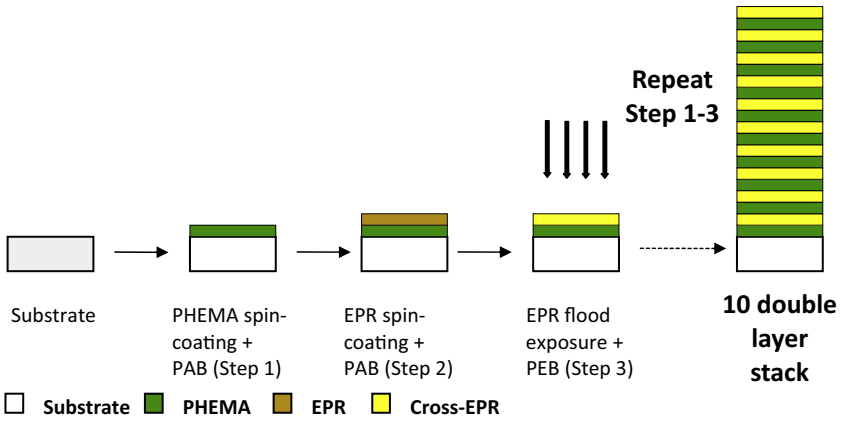

Fig. 3. 1-D PC fabrication flow chart for the application of a PHEMA/Cross-EPR bilayer. The process is applied several times in order to achieve the desired optical properties.

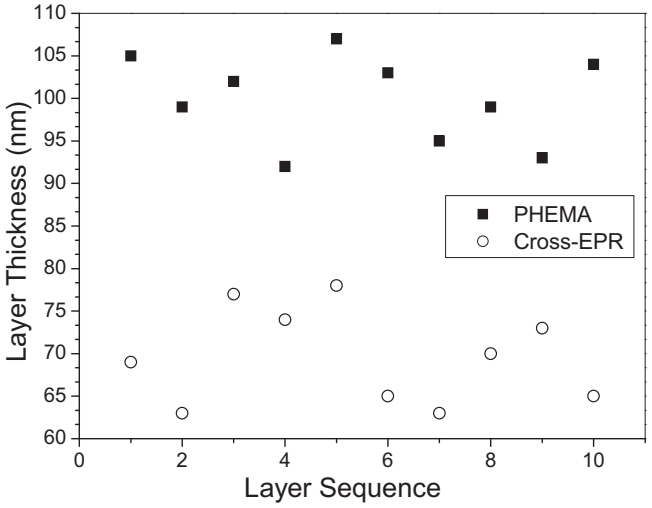

Fig. 4. Experimental polymer layer thickness distribution vs. layer location for the whole layer stack. Mean measured thickness for PHEMA is 100 nm ± 5 nm and for Cross-EPR is 70 nm ± 6 nm.

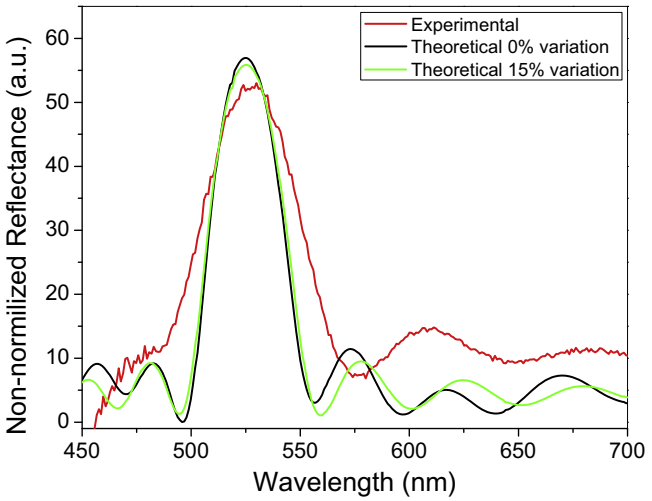

Fig. 5. Theoretical and experimental reflectance spectra of a 10 double layer PHEMA/Cross-EPR stack on glass. The black line is the theoretical reflectance curve with zero dispersion in thickness of both layers while the green line is the theoretical reflectance spectrum for layer thicknesses with 15% deviation. (For interpretation of the references to color in this figure legend, the reader is referred to the web version of this article.)

very good agreement with the theoretical one when considering layers with zero layer thickness tolerance i.e. all material-A layers have the same thickness (d_A) and all material-B layers have the same thickness (d_B). Therefore this characteristic allows for the high processing tolerance.

3.3. Humidity sensor

For the evaluation of the humidity sensing performance of the 1-D PC, the reflectance spectra of the samples were recorded by an experimental set-up being able to deliver pre-determined humidity values through mixing, at selected concentrations, water-saturated nitrogen flows with dry nitrogen flows [24]. The reflectance spectra at equilibrium are illustrated in Fig. 6a showing a linear red-shift of the reflectance peak by 62 nm from 0% to 90% RH. In the insert of Fig. 6a the dynamic measurement in terms of the reflectance peak vs. time from 0% and 90% RH is illustrated. At low humidity levels the time to reach the new equilibrium is approximately 2 min for a humidity change of 10%. At higher humidity levels the time to reach the new equilibrium is approximately 6 min for a humidity change of 20%. The relaxation time of the device, to reach 0% RH from 90% RH, is estimated 4 min approximately. The reproducibility and reversibility are illustrated in Fig. 6b. The sample was exposed in three sequential cycles each one consisting of the following steps: 0% RH, 40% RH, 0% RH and 90% RH. The response proved to be reproducible and reversible.

In order this device to operate as zero-power humidity sensor it is necessary to maximize the reflectance peak (λ_o) shift. For the reported bilayer stack this could be enhanced by careful tuning film thickness, taking into account that the reflectance peak at both relative humidity extrema should be in the visible range. From Eq. (1) it becomes obvious that in order to increase the reflectance peak shift due to humidity, the PHEMA film thickness should increase whereas the Cross-EPR decrease in order to keep the reflectance peak shift in the visible range. By considering 40 nm as the lower thickness limit for reliable and reproducible application through spin-coating of high quality polymeric film, PHEMA film thickness should be 140 nm. Furthermore this decrease in Cross-EPR film thickness would allow for faster diffusion of water molecules to the hydrophilic PHEMA layers.

In Fig. 7a the reflectance peak shift for various combinations of PHEMA/Cross-EPR film thicknesses is illustrated. Film thicknesses have been carefully selected in order that the reflectance peak at nitrogen to be nearly the same for all cases. Clearly the increase of PHEMA film thickness provide of larger reflectance peak shift for the same humidity change. Furthermore, in Fig. 7b the SEM cross-section image of a 1-D photonic crystal fabricated from

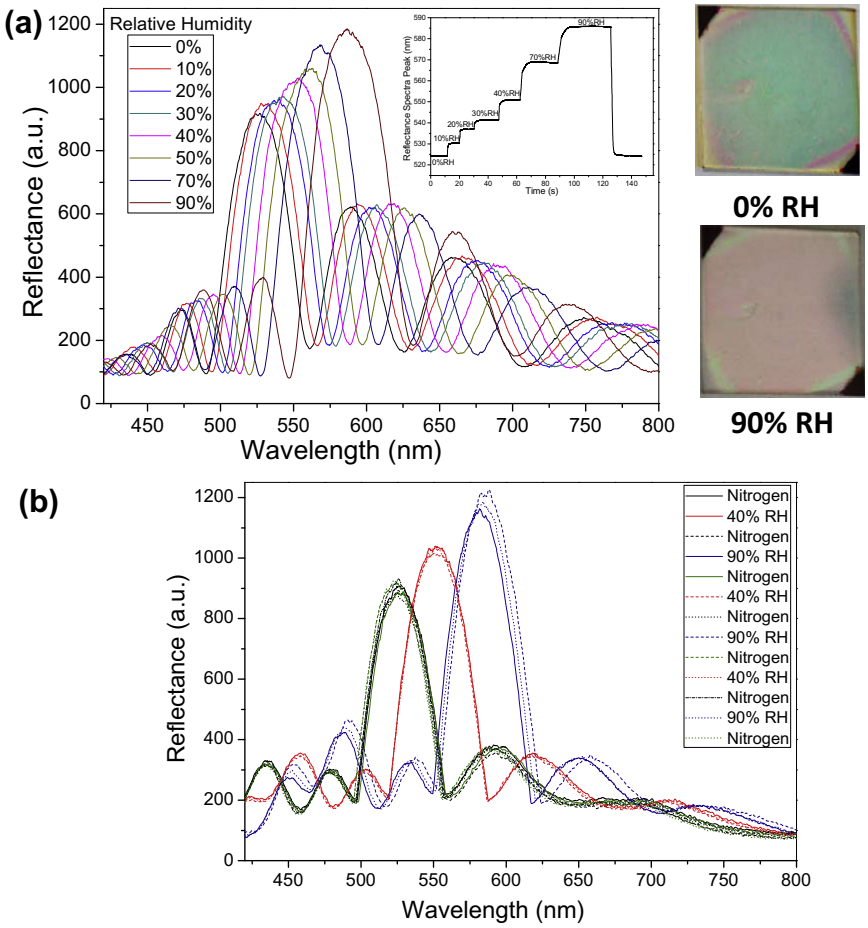

Fig. 6. (a) Reflectance spectra (raw data) as recorded by an FR-Basic tool operating in the 420–800 nm spectrum. Increase of humidity level in the environment causes swelling of hydrophilic PHEMA and thus red-shift of the reflectance peak. The spectrometer embedded in the FR-Basic tools presents increased efficiency as we move from blue part to the red part of the spectrum and for that reason the reflectance intensity increases along with humidity. In the insert the dynamic measurement in terms of the reflectance peak vs. time from 0% to 90% RH is illustrated. (b) Reflectance spectra from the sample exposed in three sequential cycles each one consisting of the following steps: 0% RH, 40% RH, 0% RH, 90% RH. The response proved to be reproducible and reversible. (For interpretation of the references to color in this figure legend, the reader is referred to the web version of this article.)

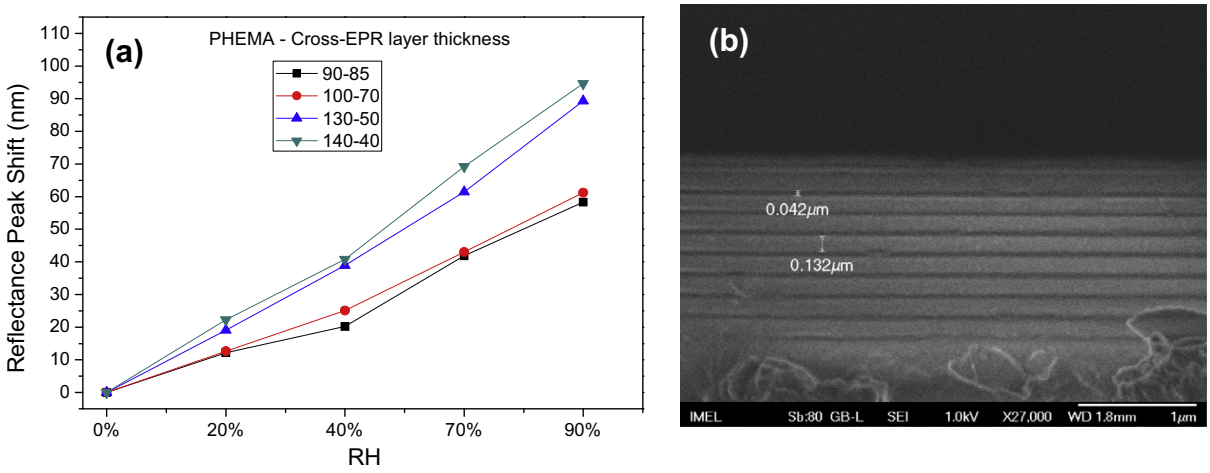

Fig. 7. (a) Effect of layer thickness of both PHEMA and Cross-EPR for various combinations aiming at similar wavelength of the reflectance peak (λ_0) at dry environment. Apparently increase of PHEMA film thickness is associated with decrease of Cross-EPR layer thickness in order to keep the reflectance peak at the 520–550 nm part of the spectrum. The increased layer thickness of the hydrophilic material causes enhanced responses in terms of shift per humidity change. In all cases the spectral shift is linear in respect to the humidity level revealing a linear swelling of PHEMA layers. (b) Cross-section SEM image of the photonic crystal on a glass slide made by PHEMA/Cross-EPR layers with nominal thickness of 140 and 40 nm respectively.

PHEMA/Cross-EPR layers with 140 and 40 nm nominal thicknesses is illustrated. The interface between the individual polymeric layers is clearly seen.

4. Conclusion

A one-dimensional polymeric photonic crystal (1-D PC) has been developed and evaluated for humidity sensing. The PC is fabricated by spin coating of sequential hydrophilic (PHEMA) and hydrophobic (crosslinked EPR) layers resulting in a reflectance peak at a wavelength defined by refractive indices and thicknesses of layers. In the presence of humidity, the hydrophobic layers remain unchanged while the hydrophilic layers absorb water molecules and swell. This swelling causes film thickness increase and shift of the reflectance peak to higher wavelengths. That way the color of the PC represents the humidity level of the environment without any need of power. Since the swelling process is based on physisorption, the whole phenomenon is reversible and reproducible.

Acknowledgements

The research was carried out partially with the equipment purchased thanks to the financial support of the European Regional Development Fund in the framework of the Polish Innovation Economy Operational Program (contract no. POIG.02.01.00-12-023/08).

References

[1] E. Yablonovitch, Phys. Rev. Lett. 58 (1987) 2059–2062.
[2] J.D. Joannopoulos, S.G. Johnson, J.N. Winn, R.D. Meade, Photonic Crystals. Molding the Flow of Light, second ed., Princeton University Press, 2008.
[3] J. Ge, Y. Yin, Angew. Chem. 50 (2011) 1492–1522.
[4] B. Gauvreau, N. Guo, K. Schicker, K. Stoeffler, F. Boismenu, A. Ajji, R. Wingfield, C. Dubois, M. Skorobogatiy, Opt. Express 16 (2008) 15677–15693.
[5] G.A. Ozin, A.C. Arsenault, Mater. Today 11 (2008) 44–51.
[6] Y. Fink, J.N. Winn, S. Fan, C. Chen, J. Michel, J.D. Joannopoulos, E.L. Thomas, Science 282 (1998) 1679–1682.
[7] J.C. Knight, Nature 424 (2003) 847–851.
[8] P. Russell, Science 299 (2003) 358–362.
[9] T. Alfrey, E.F. Gurnee, W.J. Schrenk, Polymer Eng. Sci. 9 (1969) 400–404.
[10] R.V. Nair, R. Vijaya, Prog. Quant. Electron. 34 (2010) 89–134.
[11] T. Kazmierczak, H. Song, A. Hiltner, E. Baer, Macromol. Rapid Comm. 28 (2007) 2210–2216.
[12] J. Bailey, J.S. Sharp, Eur. Phys. J. E 33 (2010) 41–49.
[13] S. Machida, T. Sugihara, S. Masuo, A. Itaya, Thin Solid Films 516 (2008) 2382–2386.
[14] M.R. Shamshiri, A.A. Yousefi, F. Ameri, J. Appl. Polym. Sci. 128 (2012) 1740–1745.
[15] L. Gonzalez-Garcia, G. Lozano, A. Barranco, H. Mıguez, A.R. Gonzalez-Elipe, J. Mater. Chem. 20 (2010) 6408–6412.
[16] A.C. Edrington, A.M. Urbas, P. DeRege, C.X. Chen, T.M. Swager, N. Hadjichristidis, M. Xenidou, L.J. Fetters, J.D. Joannopoulos, Y. Fink, E.L. Thomas, Adv. Mater. 13 (2001) 421–425.
[17] Z. Wang, J. Zhang, Z. Xie, Y. Wang, J. Yin, Y. Li, S. Li, L. Liang, L. Zhang, H. Cui, J. Mater. Chem. 22 (2012) 7887–7893.
[18] E. Tian, J. Wang, Y. Zheng, Y. Song, L. Jiang, D. Zhu, J. Mater. Chem. 18 (2008) 1116–1122.
[19] M. Vasilopoulou, S. Boyatzis, I. Raptis, D. Dimotikalli, P. Argitis, J. Mater. Chem. 14 (2004) 3312–3320.
[20] M. Kitsara, D. Goustouridis, S. Chatzandroulis, M. Chatzichristidi, I. Raptis, T.H. Ganetsos, R. Igreja, C.J. Dias, Single chip interdigitated electrode capacitive chemical sensor arrays, Sens. Act. 127 (2007) 186–192.
[21] K. Manoli, P. Oikonomou, E. Valamontes, I. Raptis, M. Sanopoulou, J. Appl. Polym. Sci. 125 (2012) 2577–2584.
[22] M. Chatzichristidi, I. Raptis, P. Argitis, J. Everett, J. Vac. Sci. Technol. B 20 (2002) 2968–2972.
[23] M. Chatzichristidi, I. Raptis, C.D. Diakoumakos, N. Glezos, P. Argitis, M. Sanopoulou, Microelectron. Eng. 61–62 (2002) 729.
[24] K. Manoli, D. Goustouridis, S. Chatzandroulis, I. Raptis, E.S. Valamontes, M. Sanopoulou, Polymer 47 (2006) 6117–6122.
[25] M. Kitsara, K. Beltsios, D. Goustouridis, S. Chatzandroulis, I. Raptis, Polymer J. 43 (2007) 4602–4612.
[26] P. Argitis, I. Raptis, C.J. Aidinis, N. Glezos, M. Baciocchi, J. Everett, M. Hatzakis, J. Vac. Sci. Technol. B 13 (1995) 3030–3034.
[27] M.-I. Georgaki, P. Oikonomou, A. Botsialas, N. Papanikolaou, I. Raptis, P. Argitis, M. Chatzichristidi, Procedia Eng. 25 (2011) 1177–1180.